Electronic Supplementary Information

One-pot Synthesis of Enzyme@Metal-Organic Materials (MOM) Biocomposites for Enzyme Biocatalysis

Yanxiong Pan,[1] Hui Li,[2] Mary Lenertz,[1] Yulun Han,[1] Angel Ugrinov,[1] Dmitri Kilin,[1] Bingcan Chen,*[,2] and Zhongyu Yang*[,1]

1. Department of Chemistry and Biochemistry, North Dakota State University, Fargo, ND, 58102
2. Department of Plant Sciences, North Dakota State University, Fargo, ND, 58102

Corresponding to: zhongyu.yang@ndsu.edu; Bingcan.chen@ndsu.edu

1. Chemicals and materials

5,5'-Dehydrodivanillate (DDVA, 95%) was purchased from Oakwood Chemicals. Calcium chloride ($CaCl_2$ anhydrous, ≥99.9%%), zinc nitrate hexahydrate ($Zn(NO_3)_2$. $6H_2O$, 98%), hydrogen peroxide (30% wt. in water), α-D-glucose, bicinchoninic acid (BCA) kit for protein concentration determination, 2,2′-azino-bis(3-ethylbenzothiazoline-6-sulfonic acid) diammonium salt (ABTS), lysozyme (lys, chicken egg white, ≥ 90%), 4-nitrophenyl acetate, amano lipase PS from Burkholderia cepacian (lipase, ≥30,000 U/g), glucose oxidase from Aspergillus niger (GOx, ≥100,000 units/g solid), peroxidase from horseradish (HRP, ≥250 units/mg solid), and micrococcus lysodeikticus (Sigma-Aldrich, ATCC No. 4698, M3770) were purchased from Sigma-Aldrich. EnzChek® Lysozyme Assay Kit was purchased from ThermoFisher Scientific. S-(2,2,5,5-tetramethyl-2,5-dihydro-1-hpyrrol-3-yl) methyl methanesulfonothioate (MTSL) was obtained from Toronto Research Chemicals. All other chemicals, such as dimethyl sulfoxide (DMSO), isopropanol, and sodium hydroxide, were of analytical grade and purchased in high purity without further purification.

2. Synthesis of enzyme @MOF composite

Synthesis of 6,6'-Dihydroxy-5,5'-dimethoxybiphenyl-3,3'-dicarboxylate sodium (Na_2-DDVA)

The synthesis of Na_2-DDVA was carried out by neutralized the DDVA with NaOH. Typically, DDVA (133.2 mg, 0.3 mmol) was dispersed in NaOH solution (700 μL, 1 M). The formed brown liquid was precipitated and washed to neutral using isopropyl alcohol, then dried in an oven at 60 °C.

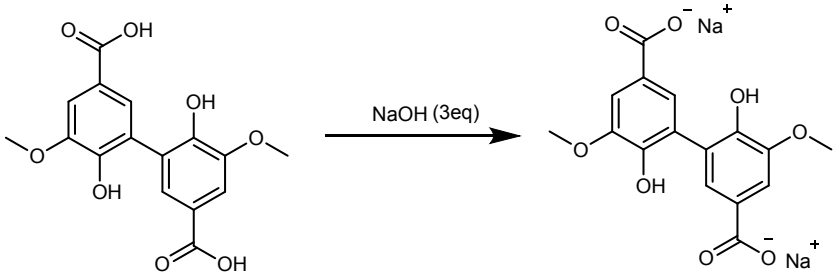

Scheme S1. Synthesis of Na_2-DDVA.

Fluorescein 5(6)-isothiocyanate (FITC) labeled enzyme

An enzyme (500 μL, 1 mM) and FITC (30 μL, 25 mM in DMSO) were diluted in 10 mL carbonate-bicarbonate buffer (50 mM, pH = 9.2) and nutated at ambient temperature for 1 h. Excess FITC was removed using the Amicon spin concentrator (Millipore, 10,000 MWCO, 50 mL). The obtained FITC-enzyme was covered with foil and stored at -4 ºC for the next steps.

Synthesis of enzyme@Ca-DDVA composites

Typically, $CaCl_2$ (40 μL, 0.5M) and an enzyme (20 μL, 1 mM) was dispersed into 50 μL double-distilled water (DD water). Then, Na_2-DDVA (25 μL, 0.5M) was dropped into the mixture and sat still under ambient temperature for 24 h. The pellets were washed with water (containing 25 mM NaCl) at least 3 times to remove unreacted species, followed by re-dispersion into 100 μL DD water and stored at -4 ℃ for further use. Single crystal of enzyme@Ca-DDVA was obtained by sealing the mixture and incubating in an oven at 60 ℃ for 24 h. Then, the monolith was picked for acquiring the x-ray diffraction (XRD) pattern. The loading efficiency

(the percentage of the loaded enzyme in the Ca-DDVA compared to the total enzyme added) is 3-10% depending on the selected enzyme (~10 % for lys, ~3 % for lipase, ~3 % for GOx, and ~4 % for HRP). The unloaded enzymes in the supernatant after co-precipitation were covered using the Amicon Centrifuge Concentrators (10 kDa cutoff) which allow the metal and ligand to flow through but keep the relatively large enzymes.

Synthesis of lys@Zn-DDVA composites

Typically, $Zn(NO_3)_2$ (25 μL, 0.5M) and an enzyme (20 μL, 1 mM) were dispersed into 1 mL DD water. Then, Na_2-DDVA (25 μL, 0.5M) was dropped into the mixture and sat still for 24 h. The pellets were washed with water (containing 25 mM NaCl) for at least 3 times, re-dispersed to 100 μL DD water, and stored in a refrigerator at 4 ℃ for further use. The loading efficiency (the percentage of the loaded enzyme in the Zn-DDVA compared to the total enzyme added) is 2-8% depending on the selected enzyme (~8 % for lys, ~2 % for lipase, ~2 % for GOx, and ~3 % for HRP). The unloaded enzymes in the supernatant after co-precipitation were covered using the Amicon Centrifuge Concentrators (10 kDa cutoff) which allow the metal and ligand to flow through but keep the relatively large enzymes.

3. Characterization

Scanning electron microscope (SEM)

Morphology of the lys@MOFs were measured using a JEOL JSM-7600F scanning electron microscope (JEOL USA Inc., Peabody, Massachusetts) operating at 2 kV. Typically, dried samples were mounted on aluminum mounts using carbon adhesive tabs/tape and then coated with a conductive layer of carbon in a high-vacuum evaporative coater (Cressington 208c, Ted Pella Inc., Redding, California, USA).

Powder X-ray Diffraction (PXRD)

Powder XRD experiment was performed on a Single Crystal Bruker's Diffractometer, Apex 2 Duo with Cu IμS X-ray source. Detector resolution was changed to 1024 x 1024 pixels. The data collection strategy is shown in Table S1. Images were unwrapped, converted, and integrated with Apex 3 v. 2017.3-0. The final phase analysis was performed on the PAnalytical X'Pert HighScore software.

Thermogravimetric analysis (TGA)

TGA was measured using a Thermogravimetric Analyzer (TGA), TA Instruments Q500. Each sample was measured between 25 °C and 900 °C at a heating rate of 10 °C/min under a 40 mL/min nitrogen flow. Prior to any measurement, the samples were dried in an oven at 110 °C to remove water or other solvents.

Confocal microscopy imaging analysis

To acquire confocal fluorescence images, FITC-enzyme@Ca-MOFs were dispersed into methanol and loaded on a Zeiss Axio observer Z1 LSM 700 confocal laser-scanning microscope (Peabody, MA). The images were processed using Imarisx64 9.0.2 software by Bitplane AG (Concord, MA).

Fourier Transformation Infrared (FTIR) spectroscopy

FTIR spectra were acquired with an FTIR spectrometer (Thermo Scientific Nicolet is-10) equipped with an Attenuated Total Reflection (ATR) element of Smart iTX AR Diamond and the

Omnic 5.1 software. The background was collected prior to running the samples and used as the baseline. Dried enzyme@MOFs and corresponding hybrids were loaded to the crystal plate and slightly pressed. Each sample was scanned 64 times with the range from 400 to 4000 cm^{-1}. Data are shown in Figure S1.

Site-Directed Spin labeling of lysozyme

Mutants of 44C, 65C, 72C, 89C, 109C, 118C, 131C, and 151C were prepared as described before.[1] Briefly, the mutants were generated by QuikChange site-directed mutagenesis of the pET11a-T4L genetic construct containing the pseudo-wild-type mutations C54T and C97A,[2, 3] followed with verification of each mutation by DNA sequencing.[4] These mutants were expressed, purified, and then desalted into a buffer suitable for spin labeling (containing 50 mM MOPS and 25 mM NaCl at pH 6.8). The desalted protein mutants were then reacted with a 10-fold molar excess of S-(2,2,5,5-tetramethyl-2,5-dihydro-1H-pyrrol-3-yl) methylmethanesulfonothioate (MTSL, Toronto Research Chemicals, Inc., Toronto) at 4°C overnight (yielding R1). Excess MTSL was removed using the Amicon spin concentrator (Millipore, 10,000 MWCO, 50 mL). The spin labeled protein mutants were stored at -20 °C for further use.

The purity of the expressed mutants was confirmed with gel-electrophoresis. As shown in Figure S2, a major band at ~18.7 kDa is consistent with the molecular weight of the protein, while the minor band at ~37 kDa is caused by partial dimerization of the mutant. Besides these two peaks, no other band is visible.

Circular Dichroism data of the spin labeled lysozyme

The secondary structures of 3 representative mutants was confirmed with Circular Dichroism (CD) and shown in Figure S3. As compared to the wildtype protein, all mutants show identical CD spectra, indicating the mutations did not influence the secondary structure of the protein.

Activity of the spin labeled lysozyme

All mutants were also confirmed to be functionally active with the same commercial activity kit (Micrococcus lysodeikticus, ATCC No. 4698, Sigma-Aldrich) wherein the bacterial cell walls were mixed with lys and the optical density at 450 nm (OD450) was monitored. A drop in OD450 indicates cell wall breakage by functional lys. As shown in Figure S4, the three mutants show a similar capability to drop the OD450. The "control" was water which does not influence the OD450.

Activity of lys@MOF

The activities of free lys and lys@MOF composites were determined using the EnzChek® Lysozyme Assay Kit (E-22013) in a 96-well plate.[5, 6] In detail, to prepare the DQ lys substrate stock suspension, 1 mL sodium azido solution (2 mM) was added into the vial of Component A of the EnzChek® Lys Assay Kit to prepare a 1mg•mL^{-1} suspension. The suspension was separated into 50 μL aliquots and stored at -20 ℃ for future use. To prepare the lys stock solution, 1 mL DD water was added into the vial of Component C (1000 U.mL^{-1}). The lys stock solution was separated into 50 μL aliquots and store at -20 ℃ for future use.

Next, a standard curve was determined for quantifying the activity. In detail, an appropriate amount of the 1X buffer (Component B in EnzChek® Lysozyme Assay Kit) was mixed with an appropriate amount of lys stock solution (1000U. mL^{-1}) so that the resultant lys concentration in the 8 wells were decreased from 500 U•mL^{-1} to 0 U•mL^{-1}. Then, the DQ lys substrate working

suspension (50 μL, 50 mg. mL^{-1}) was transferred in each well, followed by recording the fluorescence emission at ~518 nm after incubated at 37 ℃ for 30 min. The obtained standard curve is shown in Figure S5.

The activity of lys@Ca-DDVA was determined similarly. Typically, 10 μL lys@Ca-DDVA was dispersed into 490 μL HEPES buffer (25 mM, pH 7.0, 25 mM NaCl, and 2.5 mM $CaCl_2$), 50 μL of which was then mixed with 100 μL DQ lys substrate working suspension in the same buffer (25 μg• mL^{-1}). The plate was incubated at 37 ℃ and the fluorescence emission at ~518 nm was recorded in a 1-min interval using the Synergy H1 Hybrid multi-mode plate reader (Winooski, VT, USA). The activity of lys@Zn-DDVA was determined similarly. Typically, 10 μL lys@Zn-DDVA was dispersed into 490 μL HEPES buffer (25 mM, pH=7.0, 25 mM NaCl and 2.5 mM $Zn(NO_3)_2$), 50 μL of which was then mixed with the DQ lys substrate working suspension (25 μg• mL^{-1}) in the microplate wells. Then, fluorescence emission at ~518 nm was recorded.

The kinetic parameters of lys and lys@MOF were determined as reported.[5, 6] Typically, 50 μL free lys or lys@Ca/Zn-DDVA composites was transferred into the eight wells containing the corresponding HEPES buffer (see above). Then, 20 μL DQ lys substrate working suspension with increasing concentrations from 2.0 to 100 μg• mL^{-1} were added into each well. The fluorescence was recorded at 518 nm in a 1-min interval at room temperature using the Synergy H1 Hybrid multi-mode plate reader (Winooski, VT, USA). To confirm the observed activity of lys was not originated from the artifacts of MOF materials and ligand, three negative controls, the fluorescence at 518 nm of Na_2-DDVA alone, Ca-DDVA, and Zn-DDVA were recorded over time (see Figure S6).

The Michaelis constant K_m and the maximum rate constant V_{max} were determined by fitting the plot of V_0 vs [S] (see the main text) using Equation S2.[7]

υ_0 (Units/mg/min) = (ΔA * 1000)/mg (S1)

Michaelis-Menten method: $$\upsilon_0 = \frac{V_{\max}\,[S]}{K_m + [S]} \quad \text{(S2)}$$

Each repeated experiment was conducted on newly prepared composite samples and substrates.

Lipase activity

For assessing the activity of lipase immobilized on our MOFs, 10 μL of lipase@Ca-DDVA and lipase@Zn-DDVA were dispersed into ~500 μL HEPES buffer (see above). Then, 5 μL free lipase (10 μM) or lipase@Ca-DDVA were pipetted into 179.4 μL HEPES buffer (see above), followed by the addition of 16.6 μL 4-nitrophenyl acetate (10 mM in acetonitrile). The changes in absorption at 400 nm over time were recorded using the Synergy H1 Hybrid multi-mode plate reader (Winooski, VT, USA). To determine K_m and V_{max}, a series of stock solutions of 4-nitrophenyl acetate (from 0.25 to 10.0 mM) were prepared via dilution with HEPES buffer. Then 20 μL 4-nitrophenyl acetate under different concentrations was pipetted into the wells that contain 175 μL HEPES buffer and 5 μL of lipase@Ca-DDVA. The absorptions at 400 nm were recorded, and the K_m and V_{max} parameters were determined following Equation S2 (see above). A similar strategy was used to acquire K_m and V_{max} of lipase@Zn-DDVA. Similar negative controls were conducted to confirm the observed lipase activity was not originated from the artifacts of MOF materials (see Figure S7).

GOx activity

The activities of free GOx, GOx@Ca-DDVA, and GOx@Zn-DDVA were determined via the colorimetric reaction involving HRP and $ABTS^{2-}$. Specifically, 4 μL of free GOx (250 nM), GOx@Ca-DDVA (dispersed in ~500 μL HEPES buffer; see above), and GOx@Zn-DDVA (dispersed in ~500 μL HEPES buffer; see above), were mixed with 5 μL ABST (100 mM), 1 μL glucose (200 mM), 0.8 μL HRP (5 μM), and 189.2 μL HEPES. The final volume of mixture in each well is 200 μL with the final concentrations of ABST, glucose, and HRP of 2.5 mM, 1 mM, and 20 nM, respectively. The absorption change over time at 415 nm was monitored using the Synergy H1 Hybrid multi-mode plate reader (Winooski, VT, USA). The concentration of the formed $ABTS^{+\bullet}$, which can be calculated via the Beer-Lambert law, reflected the activity of entrapped GOx. Similar negative controls were conducted to confirm the observed GOx activity was not originated from the artifacts of MOF materials.

To determine the V_{max} and K_m of free GOx and GOx@Ca-MOF, eight stock solutions (80 μL) containing different amounts of glucose (from 2.5 to 80 mM) and the same amounts of ABTS (25 mM) and HRP (200 nM) were prepared. Then, 15 μL of each stock solution was simultaneously pipped into eight wells containing 180 μL HEPES buffer and 5 μL GOx@Ca-MOF using an 8-channel pipette. The final concentration of glucose ranged from 0.188 to 6 mM. The absorption at 415 nm over time was recorded in a 1-min interval using the Synergy H1 Hybrid multi-mode plate reader (Winooski, VT, USA). The K_m and V_{max} were calculated following Equation S2.

HRP activity

For assessing the activity of HRP, 10 μL of HRP@Ca-DDVA and HRP@Zn-DDVA were redispersed into 500 μL HEPES buffer. The activity assay of free HRP is similar to that of GOx except using H_2O_2 as the substrate. Typically, 4 μL HRP (250 nM), 5 μL ABST (100 mM), and 1 μL H_2O_2 (50 mM) were mixed in 190 μL HEPES buffer (see above). The final volume is 200 μL and the final concentrations of ABST and H_2O_2 are 2.5 mM and 0.25 mM, respectively. The UV absorption at 415 nm was monitored over time using the Synergy H1 Hybrid multi-mode plate reader. Similar negative controls were conducted to confirm the observed HRP activity was not originated from the artifacts of MOF materials.

The V_{max} and K_m were acquired by monitoring the effect of substrate concentration on the absorption at 415 nm. Typically, eight stock solutions (120 μL) containing various amounts of H_2O_2 (from 0.833 mM to 53.33 mM) and the same amount of ABTS (33.33 mM) were prepared. 15 μL of stock solutions were simultaneously pipetted into wells containing 4 μL HPR@Ca-MOF and 190 μL HEPES buffer. The absorption at 415 nm was recorded using the Synergy H1 Hybrid multi-mode plate reader (Winooski, VT, USA) and the K_m and V_{max} were calculated following Equation S2.

The activity of GOx-HRP cascade

As-prepared GOx-HRP@Ca-DDVA and GOx-HRP@Zn-DDVA were washed and redispersed to 500 μL HEPES buffer. Then, 1 μL glucose (200 mM), 4 μL GOx-HRP@Ca-BPDC and 5 μL ABST (100 mM) were added into 190 μL HEPES buffer (25 mM, pH=7.0, 25 mM NaCl and 2.5 mM CaCl2). The UV absorption at 415 nm was monitored over time (see Figure S8)

Reusability

As representatives for the reusability test of our biocomposites, lypase@Ca-DDVA and lipase@Zn-DDVA were selected. The synthesized composites were dispersed into 100 μL HEPES buffer (see above). Then, 5 μL composites were mixed with 912 μL HEPES buffer and 83 μL 4-nitrophenyl acetate (10 mM in acetonitrile) and incubated at 37 ℃ for 15 min. Then, after centrifugation at 14,800 rpm for 2 min, ~900 μL supernatant was transferred into a cuvette and the adsorption at 400 nm was recorded using the NanoDrop UV-Vis Spectrophotometer (Thermo Scientific ND-2000 C). The residue was recentrifuged and washed with HEPES buffer, and the aforementioned process was repeated for at least five times.

Electron Paramagnetic Resonance (EPR) spectroscopy

For EPR measurements, ~ 20 μL Lys@Ca-MOFs was transferred into a borosilicate capillary tube (0.70 mm i.d./1.00 mm o.d.; Wilmad Labglass, Inc.). A Varian E-109 spectrometer equipped with a cavity resonator was used for the acquisition. All continuous wave (CW) EPR spectra were obtained with an observe power of 200 mW, a modulation frequency of 100 kHz, and a modulation amplitude of 1.0 G.

EPR spectral analysis

The CW EPR spectra were fit using the software developed by Dr. Altenbach and Prof. Hubbell at UCLA (http://www.biochemistry.ucla.edu/biochem/Faculty/Hubbell/). This program was essentially the MOMD model of the NSLS program established by Freed and co-workers.[8] In our case, the MOMD model includes three coordinate frames to describe the internal motion of the nitroxide spin label in a protein. First, the molecular frame which is consistent with the magnetic tensor (g- and hyperfine-tensor) frame (x_M, y_M, z_M). The z_M is defined as to be along with the nitroxide p orbital; the x_M is parallel with the NO bond axis; the y_M follows a right-handed coordinate system. Second, the principle frame of the rotational diffusion tensor (x_R, y_R, z_R), which usually deviate from the molecular frame. Although in principle three Euler angles are required to correlate the two frames, experiences from spectral simulations indicated that only the β_D, the angle between z_R and z_M (Figure S9), is important for simulations. Third, the coordinate frame describing the diffusion of the spin label on the attached enzyme, the director frame, (x_D, y_D, z_D). A good approximation/simplification is to allow the spin label to rotate/move freely within a cone (Figure S9). This also leads to simplifying the rotational diffusion tensor R, wherein the axial symmetry can be assumed. The angle between z_D and z_R is defined as θ.

According to Budil et al,[8] a restoring (ordering) potential (U) is appropriate to describe the extent of spatial constraints of the spin label within the "cone". The restoring potential $U(\theta) = -1/2 k_B T c_0^2 (3\cos^2\theta - 1) + H.O.T.$, where c_0^2 is a scaling coefficient and H.O.T. represents higher order terms as defined in the literature.[8] In our simulations, only the dominant term and the first H.O.T. term was involved, the coefficients of which are C_{20} and C_{22} in our simulations, respectively.

For describing the nitroxide side chains on a protein subject to the above ordering potential, the director frame is fixed. The existence of the restoring potential results in an anisotropic motion and can be characterized by the order parameter $S = -1/2 \langle(3\cos^2\theta - 1)\rangle$, where the brackets indicate spatial average. For an individual protein molecule, z_D forms an angle ψ with respect to the external magnetic field. To obtain the final spectrum corresponding to an isotropic distribution of protein orientations, the spectra are summed over ψ.

Supporting Figures

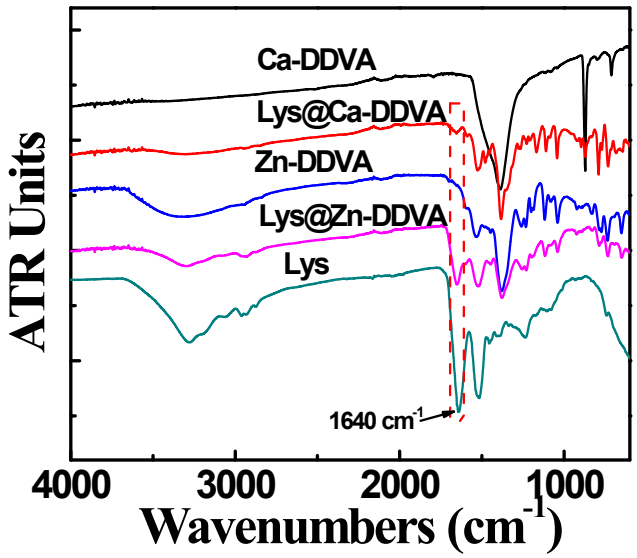

Figure S1. Fourier transform infrared (FT-IR) spectra of a representative enzyme in this study, lys, and synthesized MOFs, as well as enzyme@MOF biocomposites.

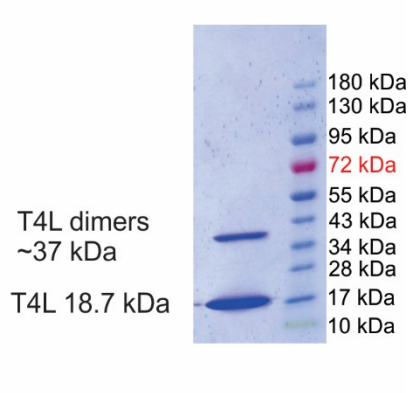

Figure S2. Gel-electrophoresis of the expressed mutants of lysozyme. Only one mutant (151R1) is shown since all mutants show identical bands.

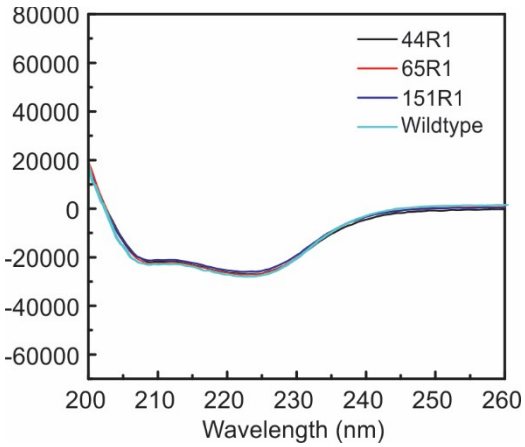

Figure S3. CD spectra of the involved mutants and the wildtype lysozyme.

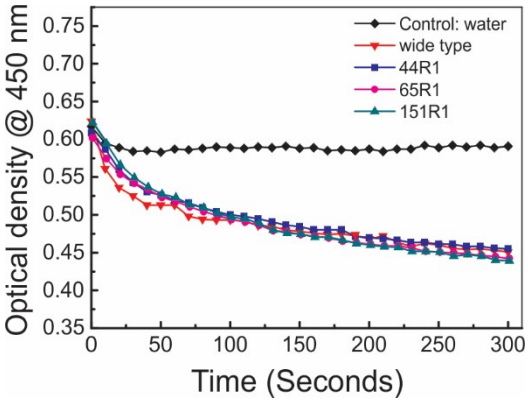

Figure S4. The activity assay of three mutants and the wildtype protein of T4L. A drop in OD450 was observed for all protein samples. The "control" was acquired by mixing water with the bacterial cell walls.

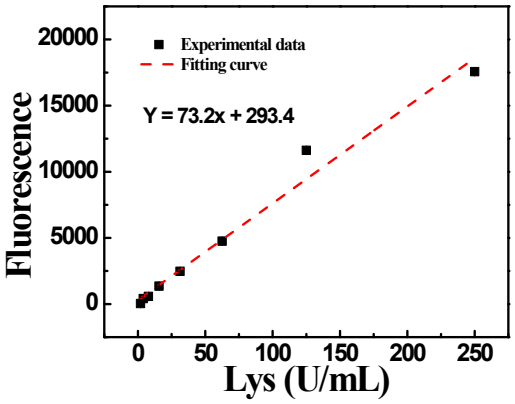

Figure S5. Standard calibration of lys activity using the EnzChek Lysozyme Assay Kit.

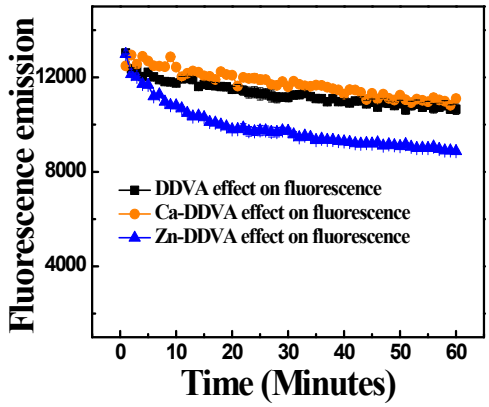

Figure S6. Negative controls of lys activity test. The slight drop in fluorescence emission is likely caused by substrates pelleting down to the bottom of the test cuvette.

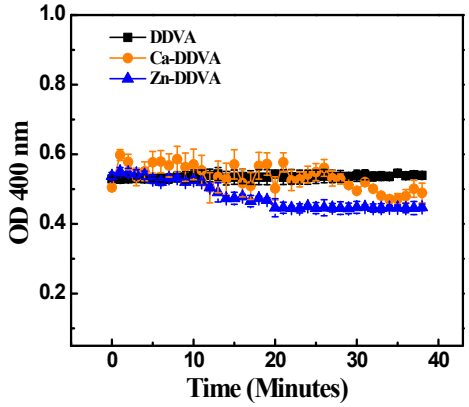

Figure S7. Negative controls of lipase activity test.

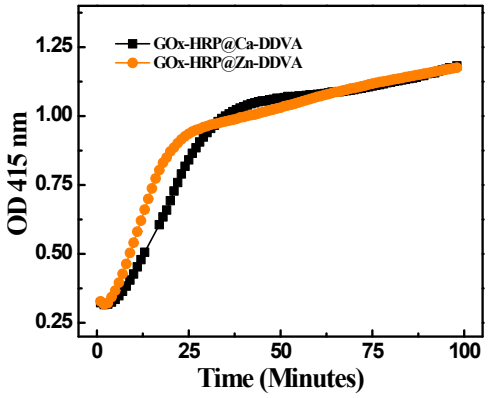

Figure S8. The cascade catalytic performance of GOx-HRP@Ca-DDVA and GOx-HRP@Zn-DDVA.

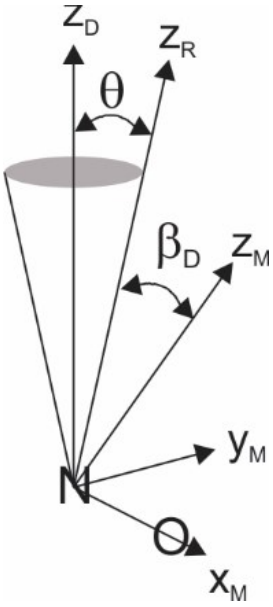

Figure S9. Definition of the three coordinate systems (Z_D, Z_R, and Z_M) related to the MOMD model used in our simulations.

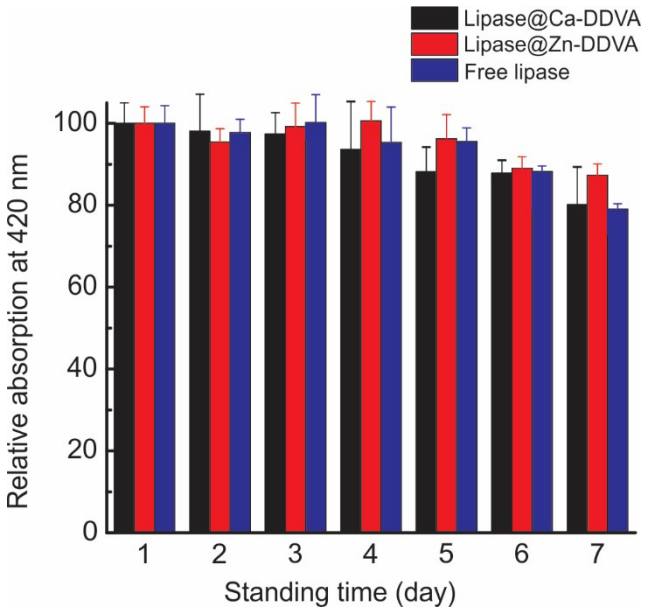

Figure S10. Relative stability (activity of samples stored on bench for multiple days) of free enzyme (purple) and upon immobilization on Ca-DDVA (black) and Zn-DDVA (red) using lipase as the representative.

Supporting Tables

Table S1. Data Collection Strategy

Run	Distance [mm]	2-theta [°]	Omega [°]	Chi [°]	Time[sec]
Phi 360	150.000	-12.000	174.000	54.720	180.00
Phi 360	150.000	-24.000	168.000	54.720	180.00
Phi 360	150.000	-36.000	162.000	54.720	180.00
Phi 360	150.000	-48.000	156.000	54.720	180.00
Phi 360	150.000	-60.000	150.000	54.720	180.00

Table S2. Selected crystallographic data of lys@Ca-DDVA

Compound	lys@Ca-DDVA
Empirical formula	$C_{32}H_{32}O_{22}Ca_3$
Formula weight	924.85
Temperature	105 K
Color	Brown
Space group	C 2/c
a (Å)	23.4643(5)
b (Å)	11.4906(2)
c (Å)	16.2903(4)
β (°)	122.775(1)
Volume ($Å^3$), z	3692.95(14)
Mu (mm^{-1})	4.776
Density (calculated) (g. cm^{-3})	1.663
F(000)	1920.0
Reflections Collected	21879
# of reflections (all)	3272
# of reflections [I>2sigma(I)]	3033
Theta range for data collection	4 to 67
Completeness to theta 66.703	99.9%
Refinement method	XL
Final R indices [I>2sigma(I)]	R1 = 0.0345, wR2 = 0.0891

R indices (all data)	R1 = 0.0374, wR2 = 0.0909

Table S3. Best fitting parameters for each labelled mutant on Ca-DDVA.

	$R_{z,\,im}$[a]	$R_{z,m}$[a]	$R_{2,im}$	$R_{2,m}$	$C_{20,im}$	$C_{22,im}$	$C_{20,m}$	$C_{22,m}$	m%	χ^2
44R1	5.99	7.05	0.88	1.57	45.8	-45.7	19.5	3.69	47.9	$3.3e^{-5}$
65R1	5.98	7.34	1.18	1.26	41.2	-41.3	9.87	4.7	58.5	$1.8e^{-5}$
72R1	6.06	7.12	1.14	1.34	41.1	-41.6	26.6	3.00	52.8	$1.4e^{-5}$
89R1	6.18	7.48	0.57	1.25	38.7	-41.9	22.3	-3.51	37.5	$1.5e^{-5}$
109R1	6.19	7.27	1.03	1.39	38.8	-42.0	27.4	-2.39	40.3	$4.9e^{-6}$
118R1	6.12	7.14	1.10	1.49	40.3	-40.8	29.2	1.21	53.1	$7.9e^{-6}$
151R1	6.02	7.07	1.19	1.54	40.2	-40.6	26.5	0.19	60.2	$1.9e^{-5}$

[a] Subscripts "im" and "m" indicate the immobile and mobile components, respectively, obtained in the simulations. Cyan indicates the representative of the N-terminus has a high chance of exposure to the solvents, leading to reduced catalytic activity in Ca-DDVA as compared to that on Zn-DDVA.

Table S4. Best fitting parameters for each labelled mutant on Zn-DDVA.

	$R_{z,\,im}$[a]	$R_{z,m}$[a]	$R_{2,im}$	$R_{2,m}$	$C_{20,im}$	$C_{22,im}$	$C_{20,m}$	$C_{22,m}$	m%	χ^2
44R1	6.05	7.05	1.27	1.53	48.1	-45.9	35.5	-1.72	28.0	$1.5e^{-5}$
65R1	5.76	7.23	1.58	1.31	50.7	-46.8	10.8	1.17	49.2	$1.9e^{-5}$
72R1	5.81	6.97	1.50	1.68	50.7	-45.8	24.5	1.91	48.4	$1.3e^{-5}$
89R1	5.63	7.26	2.03	1.27	51.1	-45.3	12.1	1.29	55.7	$1.2e^{-5}$
109R1	5.77	7.35	2.00	1.38	51.0	-44.9	6.65	0.23	50.0	$1.79e^{-5}$
118R1	5.82	7.38	1.80	1.42	51.3	-44.5	11.1	5.19	58.0	$1.78e^{-5}$

151R1	5.83	7.13	1.23	2.14	46.5	-46.5	9.52	7.76	65.2	$1.01e^{-5}$

[a] Subscripts "im" and "m" indicate the immobile and mobile components, respectively, obtained in the simulations. Yellow highlights indicate the sites that face a higher degree of restriction under the MOF crystal, possibly leading to the reduced catalytic activity on Zn-DDVA. Cyan indicates the representative of the N-terminus has a low chance of exposure to the solvents, leading to reduced catalytic activity on Zn-DDVA as compared to that on Ca-DDVA.

References:

1. Z. Yang, G. Jiménez-Osés, C. J. López, M. D. Bridges, K. N. Houk and W. L. Hubbell, *J. Am. Chem. Soc.,* 2014, **136**, 15356-15365.
2. C. J. López, M. R. Fleissner, Z. Guo, A. K. Kusnetzow and W. L. Hubbell, *Prot. Sci.,* 2009, **18**, 1637-1652.
3. M. R. Fleissner, E. M. Brustad, T. Kálai, C. Altenbach, D. Cascio, F. B. Peters, K. Hideg, S. Peuker, P. G. Schultz and W. L. Hubbell, *Proc. Natl. Acad. Sci.,* 2009, **106**, 21637-21642.
4. M. Matsumura, J. A. Wozniak, D. P. Sun and B. W. Matthews, *J. Biol. Chem.,* 1989, **264**, 16059-16066.
5. X. Wang, N. S. Yadavalli, A. M. Laradji and S. Minko, *Macromolecules*, 2018, **51**, 5039-5047.
6. N. S. Yadavalli, N. Borodinov, C. K. Choudhury, T. Quiñones-Ruiz, A. M. Laradji, S. Tu, I. K. Lednev, O. Kuksenok, I. Luzinov and S. Minko, *ACS Cataly.*, 2017, **7**, 8675-8684.
7. H. Ikemoto, Q. Chi and J. Ulstrup, *J. Phys. Chem. C*, 2010, **114**, 16174-16180.
8. D. E. Budil, S. Lee, S. Saxena and J. H. Freed, *J. Magn. Reson. A*, 1996, **120**, 155-189.